Spatial Behavior and Long-Term Decline of Radiocesium in Green Pheasants (*Phasianus versicolor*) in Fukushima: A Left-Censored Regression Approach

Hisashi Komatsu, Kousuke Kanda, Kiemi Murakami

Fukushima Prefectural Centre for Environmental Creation, Fukushima, Japan

*Corresponding author: Hisashi Komatsu (hisashikomatsu2015@gmail.com)

Abstract

Long-term monitoring of radiocesium (^{137}Cs) in wildlife is important for assessing environmental recovery after the Fukushima Daiichi Nuclear Power Plant accident. We integrated GPS telemetry data with muscle ^{137}Cs concentrations in green pheasants (*Phasianus versicolor*) to evaluate whether observed declines in radiocesium are consistent with reduced local environmental availability. Winter telemetry indicated highly restricted movement, with 95% KDE home ranges of 1.0–7.5 ha, suggesting that muscle ^{137}Cs concentrations primarily reflect local contamination conditions. Using monitoring data from 2011–2024, the primary left-censored lognormal regression model (n = 370) estimated a significant temporal decline in muscle ^{137}Cs concentrations. This trend was supported by supplementary mixed models examining detection probability (n = 379) and concentrations among detected individuals (n = 206). These results suggest that radiocesium concentrations in green pheasants in Fukushima are declining in a manner consistent with reduced local environmental availability.

Keywords: Fukushima Daiichi Nuclear Power Plant accident, Fukushima, radiocesium, environmental monitoring, wildlife telemetry, left-censored regression, green pheasant

Introduction

Long-term monitoring of radiocesium (^{137}Cs) in wild avian populations contributes to assessing environmental recovery following the Fukushima Daiichi Nuclear Power Plant accident (Steinhauser et al., 2014). Continuous measurement of isotopic concentrations in wildlife tissues provides empirical data on the prolonged biological availability of contaminants (Beresford et al., 2016). However, interpreting spatially referenced monitoring data requires understanding the movement scales of the target species. Broadly ranging animals may accumulate radiocesium across heterogeneous contamination zones, complicating attempts to associate tissue concentrations with local environmental conditions.

The green pheasant (*Phasianus versicolor*), an endemic phasianid of Japan that exhibits territorial behavior, is a suitable species for addressing this issue (Hayashi, 2009; Matsubayashi et al., 2026). If individuals remain within localized areas, their muscle radiocesium concentrations can serve as more reliable proxies for site-specific environmental availability. Evaluating the spatial footprint of green pheasants using telemetry provides essential context for interpreting historical and ongoing monitoring data in Fukushima.

In this study, we integrated GPS telemetry with long-term radiocesium monitoring data from green pheasants in Fukushima Prefecture. Our objectives were (1) to characterize winter spatial utilization using home-range analysis, and (2) to model the temporal trajectory of ^{137}Cs concentrations using a left-censored lognormal regression framework that accounts for non-detected values without imputation (Helsel, 2012).

Methods

Study Area

Green pheasants were sampled across Fukushima Prefecture, Japan, spanning three geographic regions: Hamadori (coastal), Nakadori (central), and Aizu (western) (Figure 1). GPS telemetry was conducted in the Nihonmatsu district of Fukushima Prefecture, within the Nakadori region.

GPS Telemetry

GPS transmitters were deployed on green pheasants to evaluate winter spatial utilization. Telemetry data were processed in R using the sf package (Pebesma, 2018). Coordinates were projected to EPSG:32654 (WGS 84 / UTM zone 54N). Winter home ranges were characterized using 95% Minimum Convex Polygons (MCP; Mohr, 1947), 95% and 50% Kernel Density Estimations (KDE; Worton, 1989), and maximum linear displacements. Home-range calculations were performed using the adehabitatHR package (Calenge, 2006). Telemetry and radiocesium monitoring data were analyzed as separate domains; telemetry results provide spatial context for interpreting radiocesium trends but are not used as covariates in the concentration models.

Radiocesium Dataset

Radiocesium concentrations in green pheasant breast muscle were obtained from individuals captured under the Fukushima Prefectural monitoring program between 2011 and 2024 and measured as part of routine monitoring operations. Concentrations and sample-specific limits of detection (LOD) were standardized to a fresh-weight basis (Bq/kg). Non-detected (ND) samples were retained as left-censored observations rather than imputed as zero (Helsel, 2012). All data processing was conducted in R to derive the analytical subsets.

The primary censored analysis cohort comprised 370 individuals possessing explicit fresh-weight LODs and associated spatial metadata (Table 1). Nine ND observations lacking

sample-specific LOD records were excluded from this primary analysis. Two supplementary subsets were constructed: a binary detection model including all 379 comparable individuals, and a detected-only concentration model restricted to the 206 individuals with ^{137}Cs above LOD.

Statistical Modeling

Temporal trends in ^{137}Cs concentrations were estimated using a left-censored lognormal regression model (Therneau and Grambsch, 2000). The response variable was fresh-weight ^{137}Cs concentration. Fixed effects included years elapsed since the accident, geographic region (Hamadori, Nakadori, Aizu), and measurement mode (fresh-direct vs. dry-converted). Measurement mode was included as a methodological control term to account for differences in detection thresholds between analytical procedures, not as a biological covariate. The temporal effect was evaluated as a linear term and compared with a penalized spline parameterization to assess potential non-linearity.

A municipality-level spatial random effect could not be incorporated within the parametric survreg framework due to optimization constraints. To evaluate whether this omission affected the main inference, we constructed two supplementary mixed models: (1) a binomial GLMM predicting detection probability (n = 379) and (2) a Gaussian LMM predicting log-transformed concentrations among detected individuals (n = 206). Both models included the same fixed effects and a (1 | Municipality) random intercept (Bates et al., 2015), providing a structural check on directional consistency.

Results

Telemetry and Spatial Utilization

GPS tracking yielded sufficient positional data to characterize winter spatial utilization (Table 2). Among the four tracked females (GP45165, GP56469, GP57353, GP57354), location fixes ranged from 140–259 records, with 0–17 missing observation days (GP57354

had 17 missing days). Maximum displacements did not exceed 458 m (range: 213–458 m). KDE 95% home ranges spanned 1.0–7.5 ha, and MCP 95% areas ranged from 0.4–4.7 ha (Figure 2). One additional male (GP62487) was tracked for exploratory purposes but was treated separately from the female-centered interpretation because of sex differences and a non-overlapping tracking season (Table 2). The restricted spatial footprints of the tracked females indicate that these individuals occupied highly localized areas during winter.

Radiocesium Temporal Decline

The primary left-censored analysis included 370 individuals: 206 with detected ^{137}Cs and 164 left-censored ND observations (Table 1). Nine ND samples lacking sample-specific LODs were excluded.

The left-censored lognormal regression model estimated a significant negative effect of time on ^{137}Cs concentrations (year coefficient = −0.228, $p < 0.001$), indicating a decline over the monitoring period (Figure 3). Concentrations in Nakadori were lower than in Hamadori (coefficient = −0.957, $p < 0.001$), while Aizu did not differ significantly from Hamadori. A penalized spline for the year effect provided a slightly improved fit (effective df = 4, $p < 0.001$) compared with the linear parameterization, though both indicated a monotonic decrease.

Supplementary Mixed Models

The detection model (binomial GLMM, n = 379) estimated a significant temporal decrease in detection probability (year coefficient = −0.344, $p < 0.001$). The detected-only concentration model (Gaussian LMM, n = 206) estimated a significant temporal decrease in log-transformed ^{137}Cs concentrations (year coefficient = −0.104, $p < 0.001$). Both supplementary models, which included municipality random intercepts, yielded directionally consistent temporal and regional estimates, supporting the robustness of the primary inference.

Discussion

Our study adds an important spatial dimension to the interpretation of long-term radiocesium monitoring in wildlife. The telemetry results indicate that green pheasants, at least under the winter conditions evaluated here, used highly restricted areas, with maximum displacements of less than 460 m and 95% KDE home ranges of only 1.0–7.5 ha (Figure 2, Table 2). This spatial restriction matters radiologically because it narrows the ecological footprint over which contamination is integrated into muscle tissue. In species that range broadly across heterogeneous landscapes, tissue radiocesium can represent a composite of multiple contamination environments. In contrast, the limited winter movements observed here support the interpretation that muscle ^{137}Cs concentrations in green pheasants more closely reflect local environmental availability. From a radioecological perspective, this makes the species informative not only as a monitored organism, but also as a relatively localized biological indicator of residual forest contamination.

The temporal pattern estimated in the present study is consistent with that interpretation. The primary left-censored lognormal regression indicated a significant long-term decline in muscle ^{137}Cs, and the same directional signal was recovered in supplementary models for both detection probability and concentrations among detected individuals. Rather than viewing this simply as another demonstration that radiocesium decreases with time after the Fukushima accident, the more important implication is that the decline was observed in a species whose winter movement scale appears sufficiently limited to support local interpretation. In other words, the observed temporal decrease is consistent with a reduction in locally bioavailable ^{137}Cs, not merely with radioactive decay in the abstract. This distinction is important because wildlife monitoring is often used as evidence of ecosystem recovery, yet the ecological meaning of a tissue trend depends heavily on the movement ecology of the monitored species.

The handling of non-detects is another aspect with broader significance for environmental radioactivity studies. In long-term post-accident datasets, the proportion of non-detects

often increases as concentrations decline, making simple substitution methods increasingly problematic in later years. By retaining non-detects as left-censored observations rather than converting them to zero or an arbitrary fraction of the detection limit, the present analysis reduces the risk of downward bias in trend estimation. The supplementary models further clarify that the overall decline was expressed through two related processes: fewer individuals remaining above detection thresholds and lower concentrations among those still detected. This decomposition is useful because it shows that long-term radiological recovery in wildlife is not captured by a single summary statistic alone. Instead, it can emerge simultaneously as a shift in detectability and as a shift in the upper part of the concentration distribution.

A broader ecological interpretation emerges when these findings are viewed alongside recent long-term monitoring of wild boars in Fukushima. In wild boars, muscle ^{137}Cs showed region-specific ecological half-lives and even a transient increase in Nakadori in FY2022, and muscle concentrations were positively associated with stomach-content ^{137}Cs (Komatsu & Ikushima, 2026), highlighting the importance of dietary and other ecological drivers of short-term variation. By contrast, the green pheasants examined here showed a more spatially localized winter signal. Although these studies were not designed for direct quantitative comparison and involve different datasets, models, and species ecologies, the contrast is informative. It suggests that radiocesium trajectories in wildlife should not be interpreted as taxon-independent indicators of environmental recovery. Instead, movement scale, foraging mode, and access to soil-associated or highly contaminated food resources likely influence both the magnitude and the temporal stability of muscle contamination. In this sense, green pheasants may provide a relatively local signal of changing environmental availability, whereas wild boars may integrate broader and more variable exposure pathways across post-accident landscapes.

This interspecific contrast has practical implications for monitoring design. If the goal is to track broad regional risk in a mobile omnivore that integrates multiple dietary and habitat pathways, species such as wild boars are highly informative. If the goal is to evaluate

whether radiocesium availability is declining at a more local ecological scale, a resident ground bird with restricted winter movement may provide a different and potentially more spatially constrained line of evidence. The key point is not that one species is categorically superior to another, but that wildlife monitoring gains interpretive power when the ecology of the target species is explicitly considered. Post-accident monitoring programs are often built around sample availability and management logistics, yet our results indicate that species ecology should be treated as a central component of study design and inference.

Several limitations should be acknowledged. First, the telemetry component was based mainly on four tracked females at a focal site and during winter, so the inference regarding localized spatial use is context-specific rather than universal across all seasons, sexes, or habitats. In addition, only one male was tracked, and its tracking period did not overlap with that of the female group; generalization to sex- or season-specific differences therefore requires caution. Second, telemetry and radiocesium data were integrated conceptually rather than through an individual-level exposure model; thus, our argument is that telemetry constrains interpretation of the monitoring data, not that we directly reconstructed dose or intake histories for sampled birds. Third, the primary left-censored framework could not include a municipality random effect because of implementation constraints in survreg. However, the supplementary mixed models that incorporated municipality-level random intercepts yielded directionally consistent temporal and regional patterns, increasing confidence that the central inference does not depend on a single modeling framework.

Within those bounds, our findings support a radioecological interpretation in which muscle ^{137}Cs concentrations in green pheasants provide evidence for a long-term decline in local environmental availability in Fukushima forests. More broadly, the study illustrates that meaningful interpretation of wildlife contamination trends requires attention not only to concentration data themselves, but also to how animals move through contaminated space. Bringing together movement ecology and censored-data modeling therefore offers a useful framework for post-accident wildlife monitoring. Future work that combines seasonal telemetry, dietary information, and site-level environmental measurements would help

determine how robust this localized signal remains across seasons and habitats, and would further clarify how species-specific ecology shapes the apparent pace and variability of radiocesium decline.

Acknowledgements

We thank all collaborators who assisted with field sampling. We are also grateful to the Fukushima Prefectural staff who have continuously conducted sampling and radiocesium measurements since the Fukushima Daiichi Nuclear Power Plant accident. In addition, we thank IDEA Consultants, Inc. for their cooperation with the capture work and GPS-based investigations conducted for the home-range study.

Funding

This study was supported by the Environmental Radioactivity Research Network Center (ERAN) (Project No. P24-54).

Conflict of Interest

The authors declare no conflicts of interest.

Ethics statement

The radiocesium monitoring dataset analyzed in this study was derived from pheasants captured under the Fukushima Prefectural monitoring program and measured as part of routine monitoring operations. The authors analyzed the resulting radiocesium data and did not participate in the capture or euthanasia of birds used for the radiocesium monitoring dataset. The Fukushima Prefectural Centre for Environmental Creation does not operate an institutional animal ethics review system for field studies of this type; therefore, no institutional approval number was issued.

Permits

Capture and handling associated with the GPS telemetry survey were conducted by IDEA Consultants, Inc. For this work, IDEA Consultants, Inc. applied to the Fukushima Prefectural Nature Conservation Division for a permit for the capture of birds and mammals and the collection of bird eggs (Permit Nos. 469-1 to 469-11). In addition, prior to capture activities, a notification of temporary use of riverbed land was submitted to the Koriyama Branch Office of the Fukushima River and National Highway Office.

Table 1. Radiocesium analysis subsets

Overview of the radiocesium dataset partitioned into three analytical subsets. The primary censored analysis included all individuals with explicit fresh-weight limits of detection (LOD) and associated spatial metadata and was analyzed using a left-censored lognormal regression framework. The detection model included all comparable individuals, including non-detect samples without sample-specific LOD records, and evaluated detection probability as a binary response. The detected-only concentration model was restricted to quantified samples and analyzed log-transformed ^{137}Cs concentrations.

Analysis subset	N	Detected	Left-censored (ND)	Description
Primary censored analysis	370	206	164	All individuals with fresh-weight LOD; survreg framework
Detection model (GLMM)	379	206	173	Binary detection status including 9 ND without LOD
Detected-only concentration model (LMM)	206	206	0	Quantified samples only; log-transformed LMM

Table 2. Telemetry individual summary

GPS tracking metadata and winter home-range metrics for all collared green pheasants. MCP95, KDE95, and KDE50 are shown in hectares; maximum displacement is shown in meters. Primary indicates tracked females included in the main interpretation of winter spatial utilization, and Exploratory indicates the male shown for reference only because of sex differences and a non-overlapping tracking season.

ID	Sex	Period	Fixes	Missing d	MCP95 (ha)	KDE95	KDE50	Max disp.	Status	Note
GP45165	F	2021-11-14 to 2022-02-28	259	0	3.1	5.0	1.2	303.7	Primary	Primary female
GP56469	F	2022-11-15 to 2023-02-28	242	0	1.6	2.6	0.7	241.4	Primary	Primary female
GP57353	F	2023-11-15 to 2024-02-29	216	1	4.7	7.5	1.2	457.6	Primary	Primary female
GP57354	F	2023-11-15 to 2024-02-28	140	17	0.4	1.0	0.2	213.6	Primary	Primary female; 17 missing days
GP62487	M	2025-10-31 to 2026-02-28	360	0	13.1	19.3	3.5	736.0	Exploratory	Exploratory male

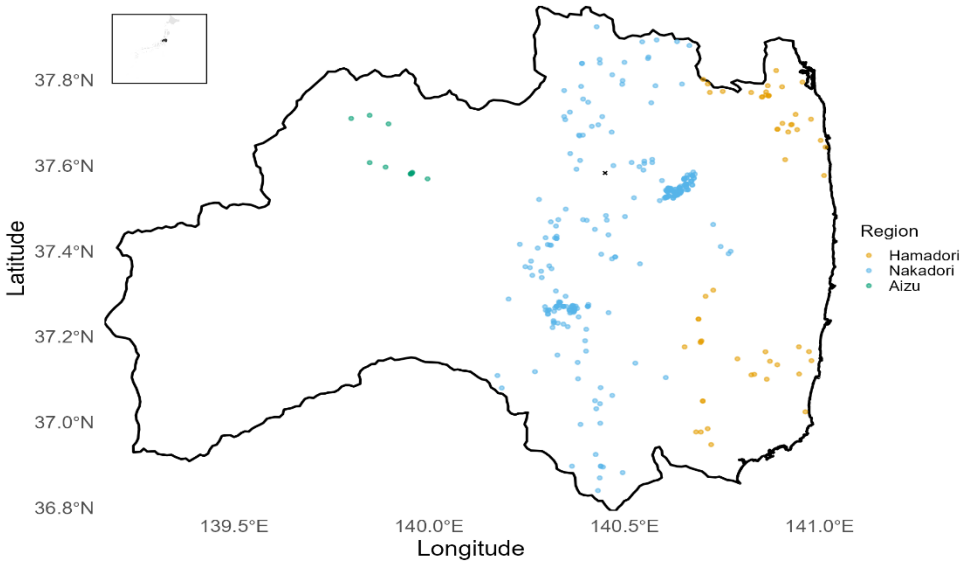

Figure 1. Study area and sampling distribution.

Map of Fukushima Prefecture, Japan, showing the geographic distribution of green pheasant samples used for radiocesium analysis across three regions: Hamadori, Nakadori, and Aizu. Colored points indicate sampling locations by region, and the cross marks the focal site used for GPS telemetry. Inset: location of the study area within Japan.

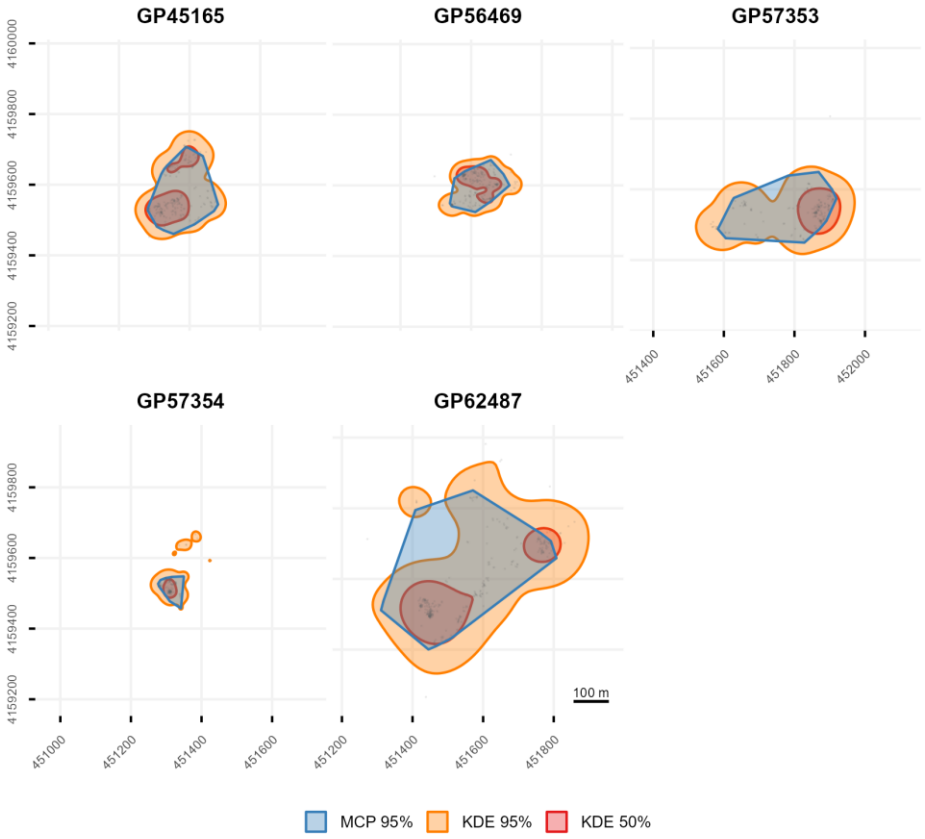

Figure 2. Winter home ranges of GPS-tracked green pheasants.

Winter space use of GPS-tracked green pheasants based on 95% minimum convex polygons (MCP95), 95% kernel density estimations (KDE95), and 50% kernel density estimations (KDE50). Gray points indicate GPS fixes. All panels share a common spatial scale to facilitate direct comparison of home-range extent among individuals. GP45165, GP56469, GP57353, and GP57354 were the tracked females used for the main spatial interpretation. GP62487 is shown as an exploratory male for reference only because of sex differences and a non-overlapping tracking season. Scale bar = 100 m.

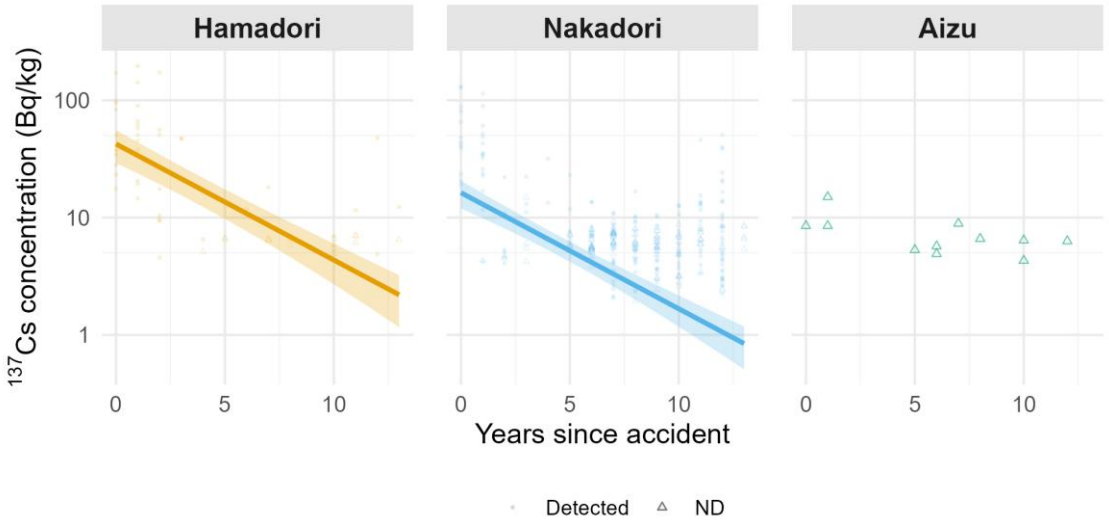

Figure 3. Long-term decline in muscle ^{137}Cs concentrations

Fresh-weight muscle ^{137}Cs concentrations (Bq/kg) in green pheasants plotted against years since the Fukushima Daiichi Nuclear Power Plant accident, faceted by region. Filled circles indicate detected concentrations, and open triangles indicate non-detect observations treated as left-censored values in the regression analysis. Solid lines and shaded bands show fitted values and 95% confidence intervals from the primary left-censored lognormal regression model. Model fits are shown for Hamadori and Nakadori; Aizu data were insufficient for fitting.

References

Bates D., Maechler M., Bolker B., Walker S. (2015). Fitting Linear Mixed-Effects Models Using lme4. Journal of Statistical Software, 67(1), 1–48. https://doi.org/10.18637/jss.v067.i01

Beresford N.A., Fesenko S., Konoplev A., Skuterud L., Smith J.T., Voigt G. (2016). Thirty years after the Chernobyl accident: What lessons have we learnt? Journal of Environmental Radioactivity, 157, 77–89. https://doi.org/10.1016/j.jenvrad.2016.02.003

Calenge C. (2006). The package “adehabitat” for the R software: A tool for the analysis of space and habitat use by animals. Ecological Modelling, 197(3–4), 516–519. https://doi.org/10.1016/j.ecolmodel.2006.03.017

Hayashi T. (2009). Individuality of crow calls in male Japanese Green Pheasants *Phasianus versicolor*. Ornithological Science, 8(1), 67–73. https://doi.org/10.2326/osj.8.67

Helsel D.R. (2012). Statistics for Censored Environmental Data Using Minitab and R (2nd ed.). John Wiley & Sons. https://doi.org/10.1002/9781118162729

Komatsu H., Ikushima S. (2026). Factors affecting log-transformed muscle ^{137}Cs concentrations in wild boars in Fukushima Prefecture over 14 years. PLOS One, 21(3), e0344189. https://doi.org/10.1371/journal.pone.0344189

Matsubayashi M., Tsuchida S., Kobayashi A., Ushida K., Shibahara T. (2026). Surveillance of gastrointestinal parasites in pheasants reared at farms and zoos in Japan: High prevalence of Eimeria species infection. Journal of Veterinary Medical Science. Advance online publication. https://doi.org/10.1292/jvms.26-0009

Mohr C.O. (1947). Table of Equivalent Populations of North American Small Mammals. American Midland Naturalist, 37(1), 223–249.

Pebesma E. (2018). Simple Features for R: Standardized Support for Spatial Vector Data. The R Journal, 10(1), 439–446. https://doi.org/10.32614/RJ-2018-009

Steinhauser G., Brandl A., Johnson T.E. (2014). Comparison of the Chernobyl and Fukushima nuclear accidents: A review of the environmental impacts. Science of the Total Environment, 470–471, 800–817. https://doi.org/10.1016/j.scitotenv.2013.10.029

Therneau T.M., Grambsch P.M. (2000). *Modeling Survival Data: Extending the Cox Model*. Springer, New York. https://doi.org/10.1007/978-1-4757-3294-8

Worton B.J. (1989). Kernel Methods for Estimating the Utilization Distribution in Home-Range Studies. Ecology, 70(1), 164–168. https://doi.org/10.2307/1938423